

## Seafloor Morphology Influences on Current Condition in a Sunda Strait Bridge Project Using Numerical Model

### *Pengaruh Morfologi Dasar Laut Terhadap Kondisi Arus pada Rencana Jembatan Selat Sunda menggunakan Model Numerik*

Franto Novico, I Nyoman Astawa, Adi Sinaga, and Arif Ali

Marine Geological Institute of Indonesia (MGI)

Jl. Dr. Junjuran No. 236, Bandung 40174, Indonesia

(Received 09 March 2015; in revised form 13 November 2015; accepted 23 November 2015)

**ABSTRACT:** It has been more than 50 years since the idea to construct the bridge of Sunda Strait was inspired by Prof. Sedyatmo. This issue is very important due to accelerate the economic growth between Sumatera Island and Java Island which is known as the densest population in Indonesia. However, until today the bridge is still not constructed yet because the high budget and the lack of technical data are still being problems. One of the most important data is current condition along the Sunda Strait. Unfortunately, no one has been clearly studied about current condition along Sunda Strait. Therefore, the information about current condition would be completed to fulfil the lack of data and information. The RV Geomarine I, as a research vessel conducted the survey in October 2012 that one of the objectives is to get the impression about the current condition around the bridge plan. Attaching echo sounder of bathy 1500 to get the depth profile and applied the RD Instrument ADCP Mobile Workhorse Monitor 300 kHz to collect the real current data and analyze the current using numerical model by Mike 21 were carried out to describe the condition of the current around the bridge proposed. In addition, the detail flexible mesh of hydrodynamic model is applied along bridge plan to analyse the current condition that caused by seafloor morphology.

Based on the ADCP data it would be seen that the highest velocity record of the current occurs at October 18<sup>th</sup> 2012 at line 19 with the value 2.63 m/sec. Nevertheless, the numerical model shown the highest current velocity occurs around the northwest of Sangiang Island where the speed attains more than 4.59 m/sec.

**Keywords:** Seafloor morphology, Sunda Strait bridge, current condition, numerical model, the Sunda Strait

**ABSTRAK:** Ide pembangunan jembatan di Selat Sunda telah ada lebih dari 50 tahun yang lalu, hal tersebut diinspirasi oleh Prof. Sedyatmo. Isu tersebut sangat penting untuk mengakselerasi pertumbuhan ekonomi di antara Pulau Sumatera dan Pulau Jawa, dimana diketahui sebagai pulau yang memiliki populasi terpadat di Indonesia. Namun, hingga saat ini jembatan tersebut masih belum terbangun disebabkan oleh masalah keuangan, dan kurangnya data teknis penunjang. Salah satu data terpenting adalah data arus di Selat Sunda. Namun, tidak ada satupun yang secara khusus melakukan penyelidikan tentang arus di sepanjang Selat Sunda. Untuk itu, informasi tentang kondisi arus akan dilakukan untuk memenuhi kekurangan data dan informasi. KR Geomarin I, sebagai kapal riset telah melakukan penelitian pada bulan oktober 2012 dimana salah satu tujuannya adalah untuk mengetahui kondisi arus di sekitar rencana jembatan. Dengan menggunakan echosounder bathy 1500 untuk mendapatkan profil kedalaman dan RD Instrument ADCP Mobile Workhorse Monitor 300 khz untuk mengumpulkan data arus sesaat dan melakukan analisa arus di sekitar rencana jembatan menggunakan model numeric Mike 21. Detail flexible mesh di sepanjang rencana jembatan diaplikasikan pada model hidrodinamika untuk menganalisa kondisi arus di sekitar area tersebut.

Berdasarkan hasil survey ADCP maka dapat diketahui nilai kecepatan air terbesar terjadi pada tanggal 18 Oktober 2012 pada lintasan 19 dengan nilai 2,63 m/det. Sementara, hasil model numeric menunjukkan nilai arus tertinggi terjadi di sekitar barat laut Pulau Sangiang dengan kecepatan lebih dari 4.59 m/det.

**Kata kunci:** Morfologi dasar laut, jembatan Selat Sunda, kondisi arus, model numeric, Selat Sunda

## INTRODUCTION

This paper would perform a description about the effect of a seafloor morphology to the water current condition, especially along a Sunda Strait Bridge Project that called Jembatan Selat Sunda (JSS).

The recent survey in Sunda Strait has been completed by Susilohadi, *et al* (2009). They focused on the sub bottom profiling to illustrate the sediment layer below seafloor. The similar topic has been finished by Gan, J, et all (2006) and Wu,, et all (2007). However, their models are applied using Princeton Ocean Model (POM) [Blumberg and Mellor, 1987] that have a curvilinear grid and usually simulate for offshore domain. However, this paper would be simulated hydrodynamic model using Mike 21 HD and applying flexible mesh to get much more refine calculation.

## METHOD

RV Geomarine I, has been accomplished the offshore survey of bathymetry, sub bottom profiling and current measurement in October 2012. Some track lines have been successfully completed to fulfil the requirements of data collection. It is not only echosounder Navisound 420 DS Reson but also bathy 1500 C SyQwest which collected bathymetry data. Based on those equipment the water depth of study area

would be illustrated and will be used as input in the numerical model. Moreover, the single channel of seismic reflection using sparker as source has been conducted in field survey, this result would be used to explain the sub bottom profiling along ADCP profile line. Additionally, a dynamic tidal current was measured by Acoustic Doppler Current Profile (ADCP) Mobile Workhorse Monitor 300 kHz in spring tide period. The current observation was focused on spring tide which it started from October 16<sup>th</sup> 2012 until 18<sup>th</sup> 2012. The vessel track is arranged from southeast to northwest direction, as can see as a red line in the Figure 1, where it connects between Sumatera and Java Islands, that the RD Instrument Acoustic Doppler Current Profile (ADCP) Mobile Workhorse Monitor 300 kHz was mounted in the RV. Geomarine I, which is connected with differential global positioning system (DGPS) and the gyro compass. As mention by King and Cooper (1993) and King, et al (1996), which the movement of shipboard should be corrected to get the good quality data. Besides, the acoustic backscatter measurement actually assumed as homogeneous current which might be reasonable in the ocean, rivers and lakes, (Gordon, 1996, Wewetzer, et al 1999; and Szupiany, et al 2007). In addition, ADCP could

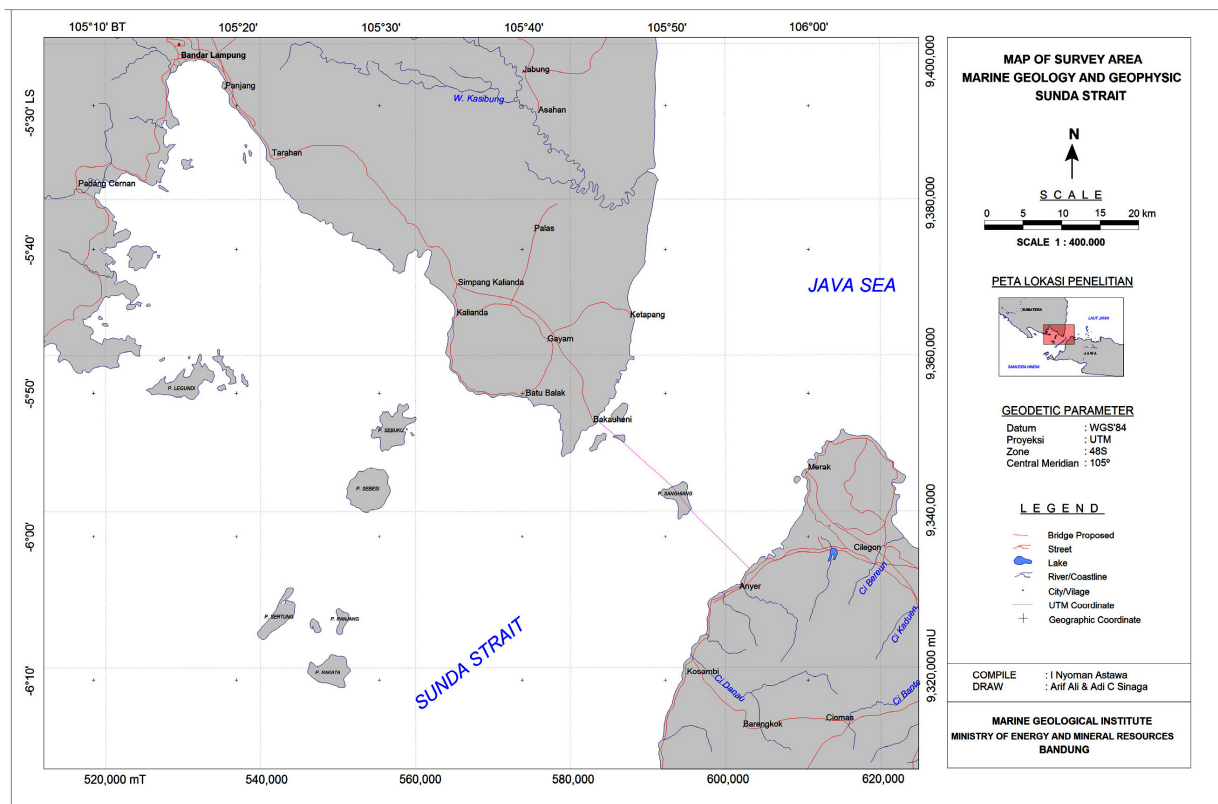


Figure 1. The area survey around bridge plan of JSS (Bridge of Sunda Strait)

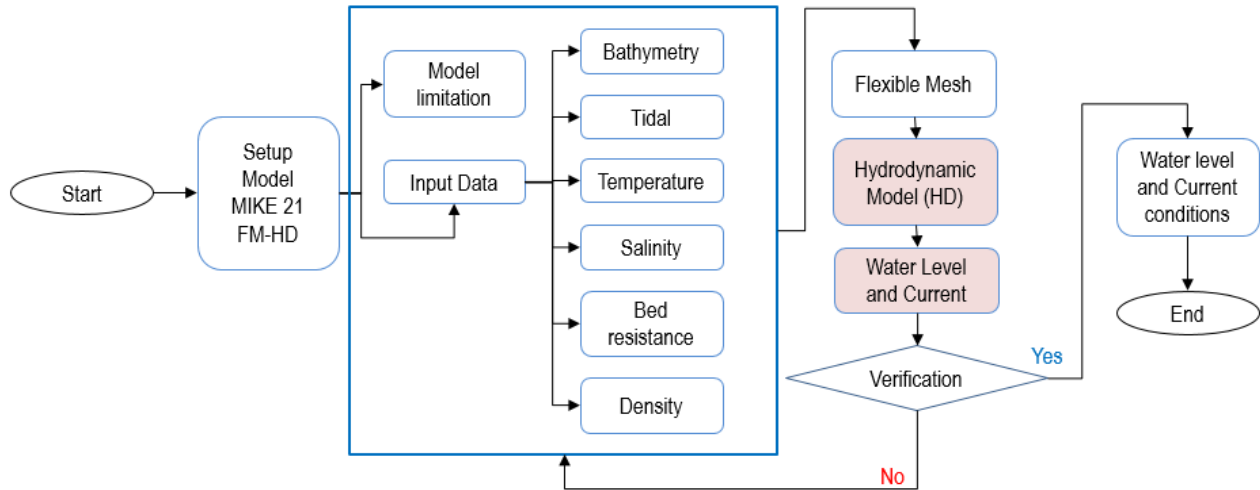


Figure 2. Flow Chart of Simulation

distinguish the habitat of seafloor such as sand, mud, sparse and dense vegetation, Warren, et al(2007).

Besides, numerical model would be simulated the impression of current condition not only along the ADCP track line but also for the area around the strait. The bathymetry data, tidal condition and some parameters would be used as input in the model. As can be seen in Figure 2, the flow chart presents some parameter where the output will be resulted in the simulation of numerical model.

In the numerical model, the grid generation is important task to computational approach. As respect to fluid mechanics, the geometry of continuum has to be described which the flow has to be modelled. It is common to create grid of rectangular or grid of triangular. However, the grids based on triangles are kindly used since they are quite flexible for adaptation to geometrically complicated situation. In this numerical model a flexible mesh is generated by using the mesh generator which creates detailed digital mesh for use in the MIKE Zero flexible mesh (FM). Within two-dimensional model the elements would be considered as triangles and quadrilateral elements. The mesh file that yielded by mesh generator is an ASCII file which includes information of the geographical position and water depth at each node point in the mesh. Mesh generators consist of three phases, a definition of the model boundaries-closed boundaries (land-water) and open boundaries, generating a depth-independent mesh and refining the mesh by scaling the element areas.

As can be seen in the Figure 3, the flexible mesh is applied in both coarse and refine flexible mesh. The refine flexible mesh is applied in the focus area of bridge plan while coarse area is applied from open boundary to the refine area. Since different interval of

bathymetry data have been collected where the dense bathymetry were collected along the bridge plan within track line interval less than 200 meter which is applied in the refine mesh while the rest of domain is applied in the coarse mesh which it has a track line within interval 500 meter to 1 km.

The system is based on the numerical solution of two/three dimensional incompressible Reynolds averaged Navier-Stokes equations invoking the assumption of Boussinesq and of hydrostatic pressure. Hence, this model consists of continuity, momentum, temperature, salinity and density equations and it is closed by a turbulent closure scheme.

Hydrodynamics approach by (DHI, 2007) describe as follow, where the shallow water equations could be presented by integration of the horizontal momentum equations and the continuity equation over depth  $h=\eta+d$

However, in numerical model of shallow water equations the integral form of the system of shallow water equations can in general form be written as

$$\frac{\partial \mathbf{U}}{\partial t} + \nabla \cdot \mathbf{F}(\mathbf{U}) = \mathbf{S}(\mathbf{U})$$

Where  $\mathbf{U}$  is the vector of conserved variables,  $\mathbf{F}$  is the flux vector function and  $\mathbf{S}$  is the vector of source terms. While, in Cartesian co-ordinates the system of 2D shallow water equations can be written below,

$$\frac{\partial \mathbf{U}}{\partial t} + \frac{\partial (\mathbf{F}_x^I - \mathbf{F}_x^V)}{\partial x} + \frac{\partial (\mathbf{F}_y^I - \mathbf{F}_y^V)}{\partial y} = \mathbf{S}$$

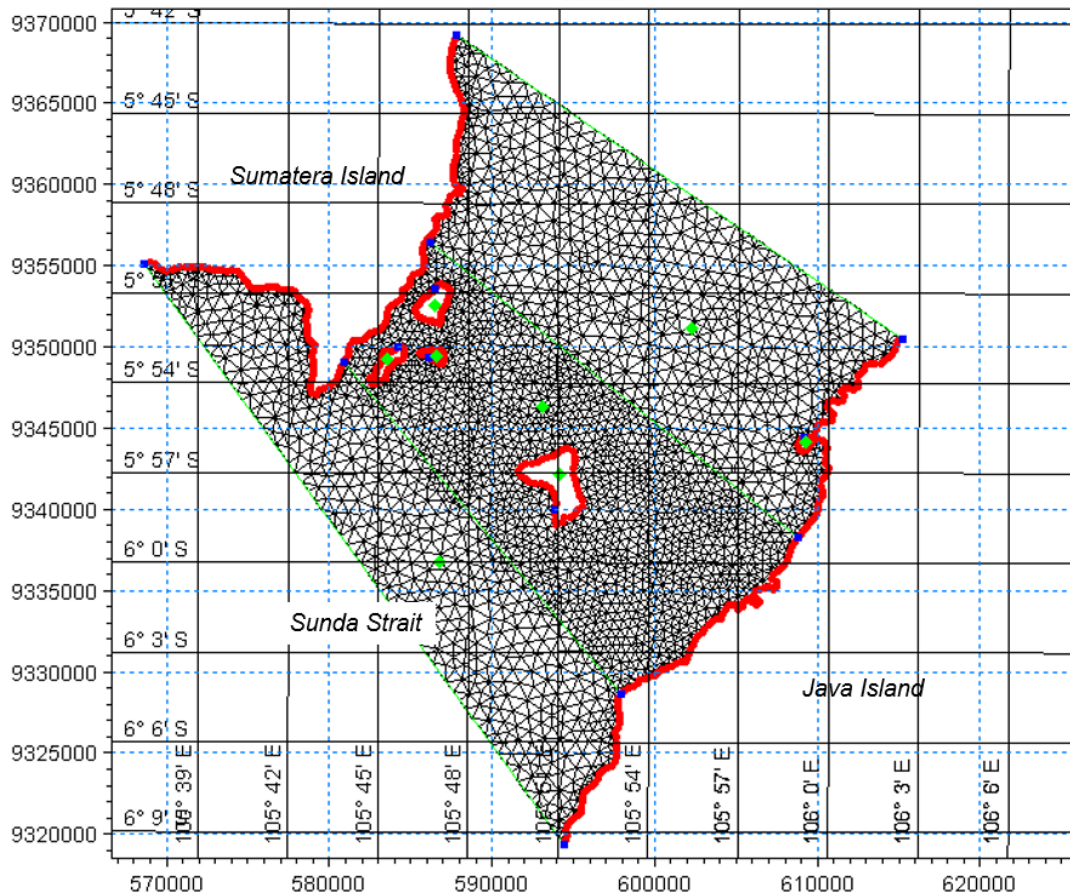


Figure 3. Mesh in the numerical model

Nevertheless, the average gradients are estimated using the approach by Jawahar, P., et al., 2000. In addition, to avoid numerical oscillations a second order TVD slope limiter (Van Leer limiter in Hirsch, 1990 and Darwish, 2003) is used. Vertical eddy viscosity would be approach by Munk-Anderson formulation (Munk, et al., 1948) and horizontal eddy viscosity would be applied by (Smagorinsky, 1963). A bottom stress is

determined by a quadratic friction law that the depth average velocity and the drag coefficient can be determined from the Chezy number,  $C$ , or the Manning number,  $M$ , however the sediment distribution map which is yielded by survey would be used to distinguish the approximately of the  $M$  value.

Tide Model Driver (TMD) as describe by Padman, L (2005) has been selected to generate tidal fluctuation

**Table 1.** Input Parameters of the models

No	Parameter	Description
1	Module	Mike 21 HD-FM, Mike 21-3 HD-FM
2	Domain	Bathymetry based on field survey
3	Simulation Period	31 days (1 <sup>st</sup> October 2012 – 31 <sup>st</sup> October 2012)
4	Time Steps	89040
5	Time Step Interval	30 sec
6	Flood and Dry	Active
7	Critical CFL Number	0.8
8	Bed Resistance	Manning N=32 and seafloor sediment distribution
9	Wind	No wind, dominant 45°, dominant 225°
10	Boundary Condition	Water Level (TMD)

in open boundaries in the north and southern part of model domain. The completely input model could be seen in Table 1. It will provide the information about all hydrodynamic parameters and mud transport parameters that analyze in the flexible model.

## RESULT

Based on the field survey, it could be clearly seen that the seafloor morphology of Sunda Strait consist of trough and ridge. As can see in southeast of the Sangiang Island which the trough reaches 130 meters depth while in northwest the ridge less than 5 meter (Figure 4). The highest ridge at northwest Sangiang Island is called 'Tugu Tiga' by people around the strait. They call tugu tiga because when the tidal is ebb three ridges will be appeared at the surface of the water. This figure presented in a radius less then 100 meters from the tugu tiga, there are found the trough at both sides north and south where the deepest of trough reach about -130 meter. Therefore, it could be imagined the effect of water current which is caused by a differences slope of seafloor morphology.

Besides, the sub bottom profiling along the ADCP track line could be seen in Figure 5. This picture proved a slope of seafloor in the northwest bigger than in the southeast. Based on geological interpretation thus the

sub bottom profiling result could be divided by 3 sequences, unit 1 is middle pleistocene, unit 2 as late pleistocene sediment and unit 3 as top pleistocene. Based on those classification so the ridge around Sangiang Island is formed by unit 2 which is defined as a sediment from the late Pleistocene. If we compare the thickness of unit 2 at northwest and southeast hence it obviously seen the high deposition is located in northwest.

The current measurement is conducted at spring condition which is started from 16<sup>th</sup> October 2012 to 18<sup>th</sup> October 2012. Within this duration, the RV. Geomarin I runs along a determined track line which is started from Java to Sumatera Islands in direction southeast-northwest and northwest-southeast. This track line is chosen by considering the nearby bridge lane, as can be seen as the red line in Figure 1.

The recorded of result data from the ADCP in spring condition would be found at the next picture. Figure 6 presents the current condition in ebb condition. In Figure 6.A, it shows the track line of RV. Geomarin I, where it moves from southeast to the northwest in 316° direction (picture left side) and northwest to the southeast in 136° direction (picture right side). In addition the sinusoidal picture in the middle illustrates the condition of tidal fluctuation which is exposed the

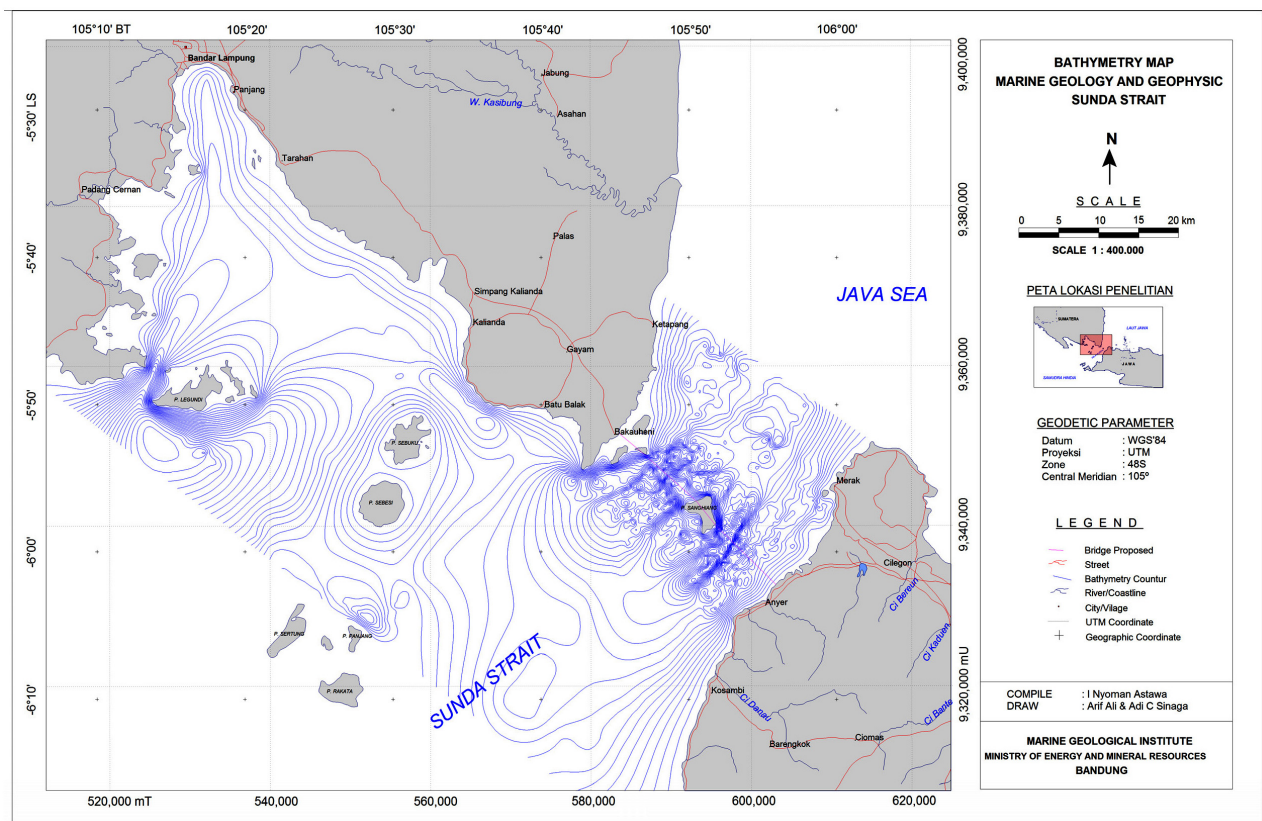


Figure 4. Bathymetry Map

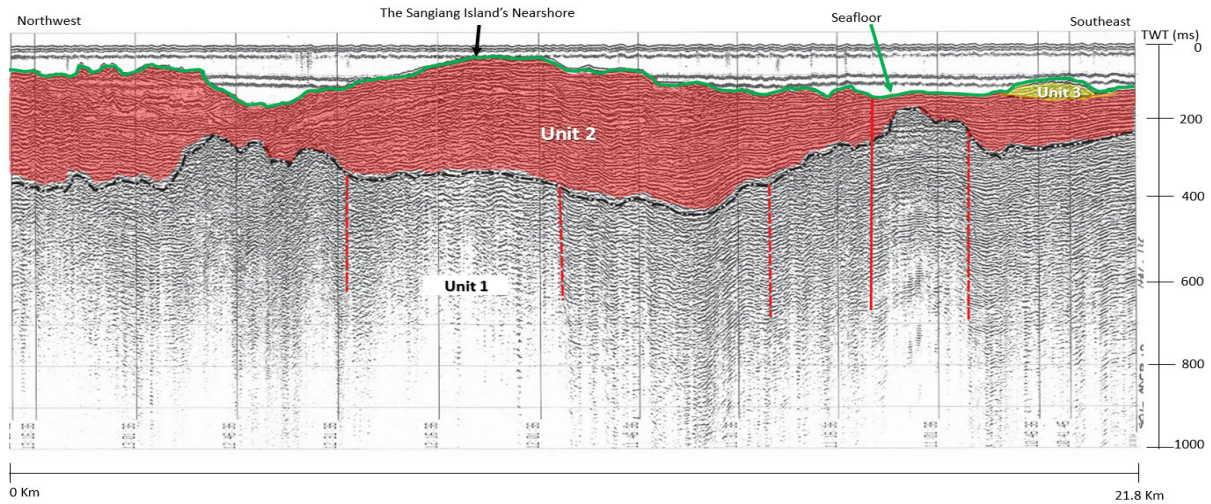


Figure 5. Sub bottom profiling condition along ADCP track line

lowest water elevation (redline). Figure 6.B displays the current speed, where in this condition both direction indicates current speed from 0.46 m/sec to 0.7 m/sec. However, in northwest-southeast track line direction the average current speed is higher than reverse direction. The dominant current direction could be found at Figure 6.C, where the dominant current direction to north and northwest is occurred at

southeast-northwest while in reverse direction the dominant current direction is southwest.

In flood condition, the current speed resulted much higher value than in ebb condition. It could be seen in Figure 7B picture to the left, which the maximum of water speed attains 1.36 m/sec (green color), it occurred when the vessel runs to the northwest. However, when the vessel runs in reversed direction the current speed has a value about 0.98 m/sec,

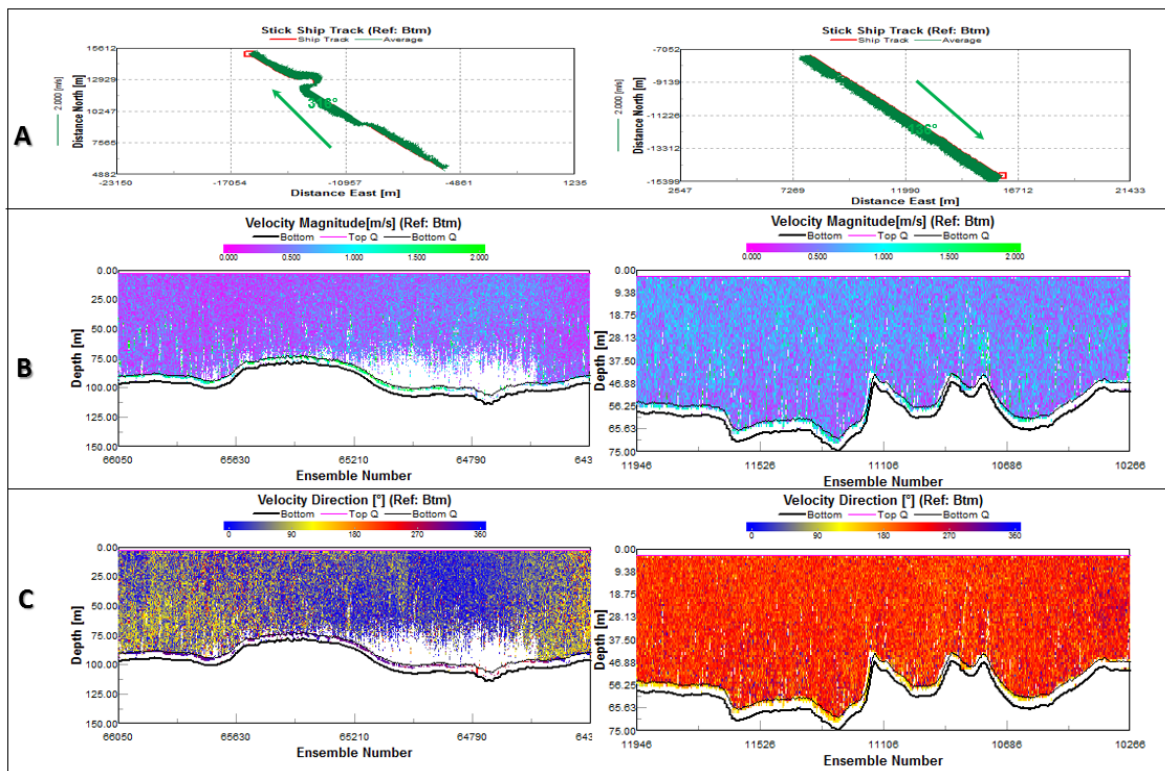


Figure 6. ADCP Recorded in spring ebb condition

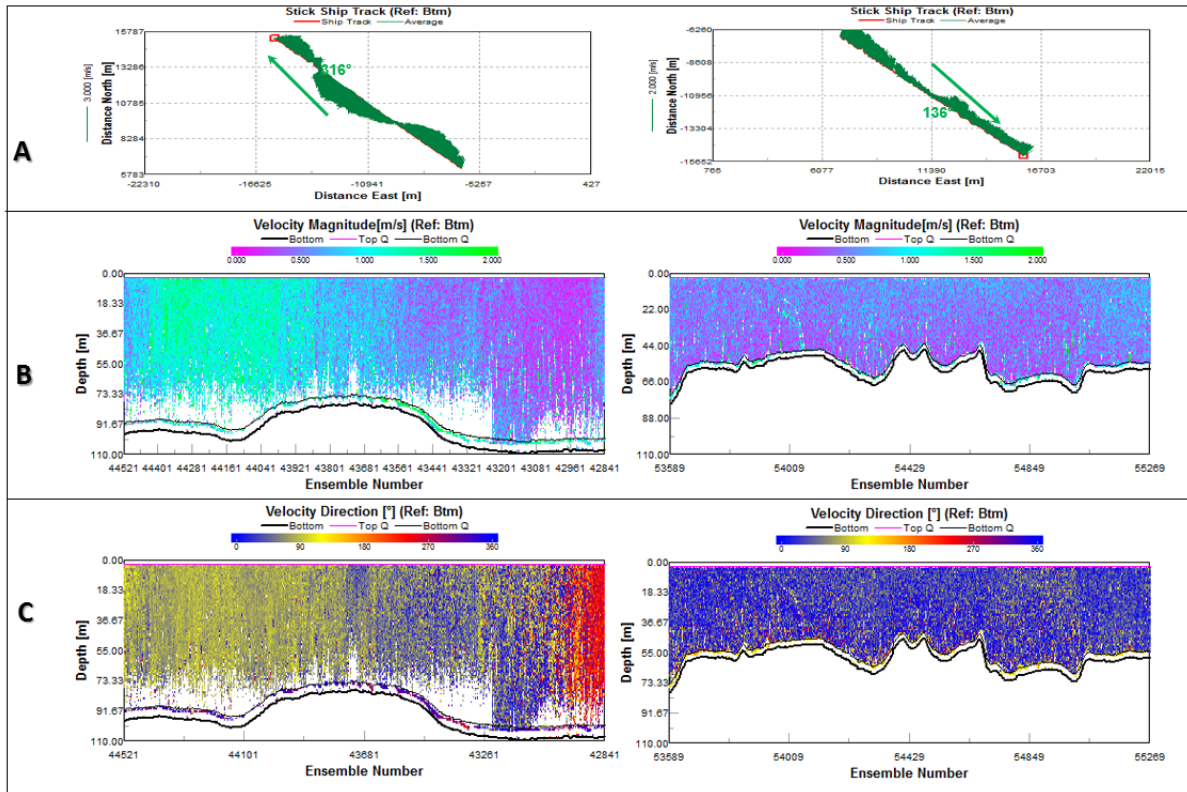


Figure 7. ADCP Data in spring flood condition

Table 2. Summary of Current Measurement in Spring Condition

No	File Name	Duration	Date	Start Time (WIB)	End Time (WIB)	Max Current Speed (m/sec)	Direction
1	Line01000r.000	10392.45	16 <sup>th</sup> Oct 2012	00:44:00	03:39:00	1.66	316°
2	Line02000r.000	13558.68	16 <sup>th</sup> Oct 2012	03:43:00	07:29:00	1.29	136°
3	Line03000r.000	10551.42	16 <sup>th</sup> Oct 2012	07:35:00	10:31:00	1.27	316°
4	Line04000r.000	10458	16 <sup>th</sup> Oct 2012	10:34:00	13:46:00	1.64	136°
5	Line05000r.000	11467.82	16 <sup>th</sup> Oct 2012	13:53:00	17:04:00	1.99	316°
6	Line06000r.000	11680.2	16 <sup>th</sup> Oct 2012	17:09:00	20:19:00	0.83	136°
7	Line07000r.000	13097.13	16 <sup>th</sup> Oct 2012	20:24:00	00:00:00	1.62	316°
8	Line08000r.000	11759.99	17 <sup>th</sup> Oct 2012	00:05:00	03:21:00	0.98	136°
9	Line09000r.000	9437.82	17 <sup>th</sup> Oct 2012	03:24:00	06:19:00	1.27	316°
10	Line10000r.000	12095.56	17 <sup>th</sup> Oct 2012	06:55:00	10:17:00	1.02	136°
11	Line01100r.000	10483.81	17 <sup>th</sup> Oct 2012	10:22:00	12:54:00	1.11	316°
12	Line01200r.000	12290.47	17 <sup>th</sup> Oct 2012	13:19:00	16:45:00	1.55	136°
13	Line01300r.000	12881.69	17 <sup>th</sup> Oct 2012	16:49:00	20:24:00	1.36	316°
14	Line01400r.000	11393.36	17 <sup>th</sup> Oct 2012	20:28:00	23:38:00	0.73	136°
15	Line01500r.000	11586.97	18 <sup>th</sup> Oct 2012	23:42:00	02:56:00	0.46	316°
16	Line01600r.000	13040.41	18 <sup>th</sup> Oct 2012	02:58:00	06:35:00	0.70	136°
17	Line01700r.000	11953.69	18 <sup>th</sup> Oct 2012	06:40:00	09:59:00	1.00	316°
18	Line01800r.000	10291.99	18 <sup>th</sup> Oct 2012	10:28:00	13:19:00	1.37	136°
19	Line01900r.000	11196.11	18 <sup>th</sup> Oct 2012	13:31:00	16:38:00	2.63	316°
20	Line02000r.000	11080.21	18 <sup>th</sup> Oct 2012	16:43:00	19:47:00	0.95	136°
21	Line21000r.000	13147.85	18 <sup>th</sup> Oct 2012	19:54:00	23:32:00	1.51	316°

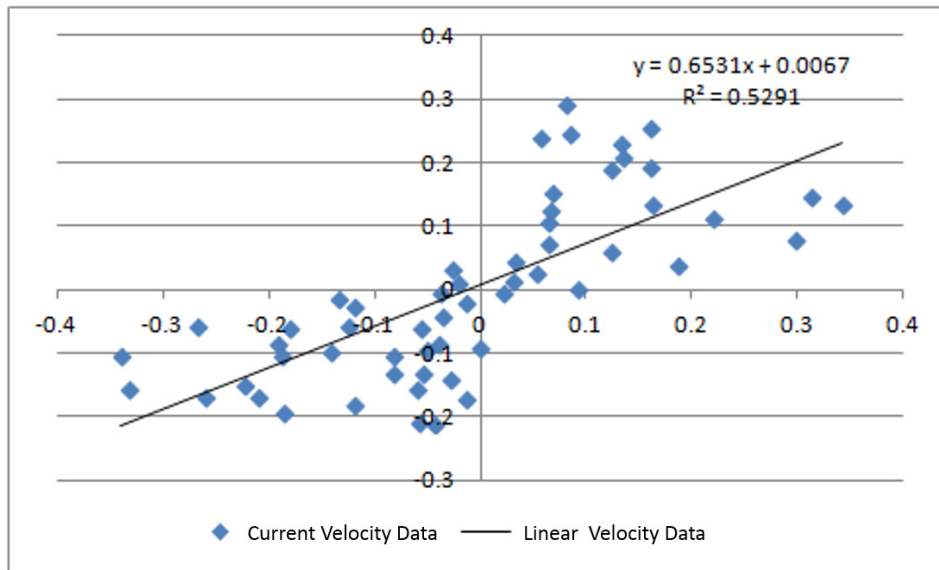


Figure 8. Verification of current data between measurement and model along ADCP track line

picture to the right. Figure 7C shows the dominant current direction is divided by 3 which are north, northeast and southeast those mean the turbulences occurred when ahead the flood time, despite the reverse direction of vessel shows a dominant current direction to southwest.

As mention before, the measurement is completed within 3 days which it has 21 recorded lines back and forth on the same transect. As described in previous figures that in the spring time, both the highest flood and the lowest ebb yielded a maximum 1.36 m/sec current speed. In fact, the highest current speed occurred at 18<sup>th</sup> October 2012, 16:30 WIB with the current velocity attains 2.63 m/sec.

## DISCUSSION

The numerical model verification has been completed as can see in Figure 8. The correlation of current velocity between ADCP data and numerical model result is about 53% that means the simulation could be continued to simulate because the correlation is above 50%. Furthermore, the model could be simulated to hindcast the current condition in neap and spring tides condition. Both tides condition of spring and neap tides would be analysed to get an impression about the current condition and especially discover the highest current velocity in the model.

### Current Condition at Flood Max in Neap Tide

Simulation model presents the current condition of flood maximum in neap tide has an average current velocity about 0.6 m/sec and the highest reaches 1.6 m/sec. Figure 9 below shows the snapshot of flood

maximum at neap condition occurred at 10<sup>th</sup> October 2012, 13:00 WIB. The distribution of surface water velocity decreases downward. From this picture, it would be said the highest current velocity occurred between the Sangiang and the Prajurit Islands, green color. The dominant of current direction is from the north-northeast to the south-southeast and in some area the whirlpool occurred that might be risky the shipping. It can be seen at northwest and southeast part of the Sangiang Island.

### Current Condition at Ebb Max in Neap Tide

At ebb, the current velocity presents an average value about 0.5 m/sec and the maximum is about 1.3 m/sec. As can see in Figure 10 which is the snapshot of ebb maximum that happened at 10<sup>th</sup> October 2012, 18:00 WIB. The distribution of surface water velocity still proved decreases downward. The location of the highest current velocity still have the similarity with the condition at flood. However, although the dominant of current direction is from the north-northeast to the south-southeast, it occurred the deflection of current direction especially in the southeast Sangiang Island that flows from northeast-southwest to northwest. Besides, the whirlpool is formed around that location, so it will be harmed the shipping.

### Current Condition at Flood Max in Spring Tide

The current of flood is occurred at 18<sup>th</sup> October 2012, 09:00 WIB. The highest current velocity still occurred between Sangiang and Prajurit Islands, within average current velocity about 1.1 m/sec and the maximum is more than 1.9 m/sec. A description of



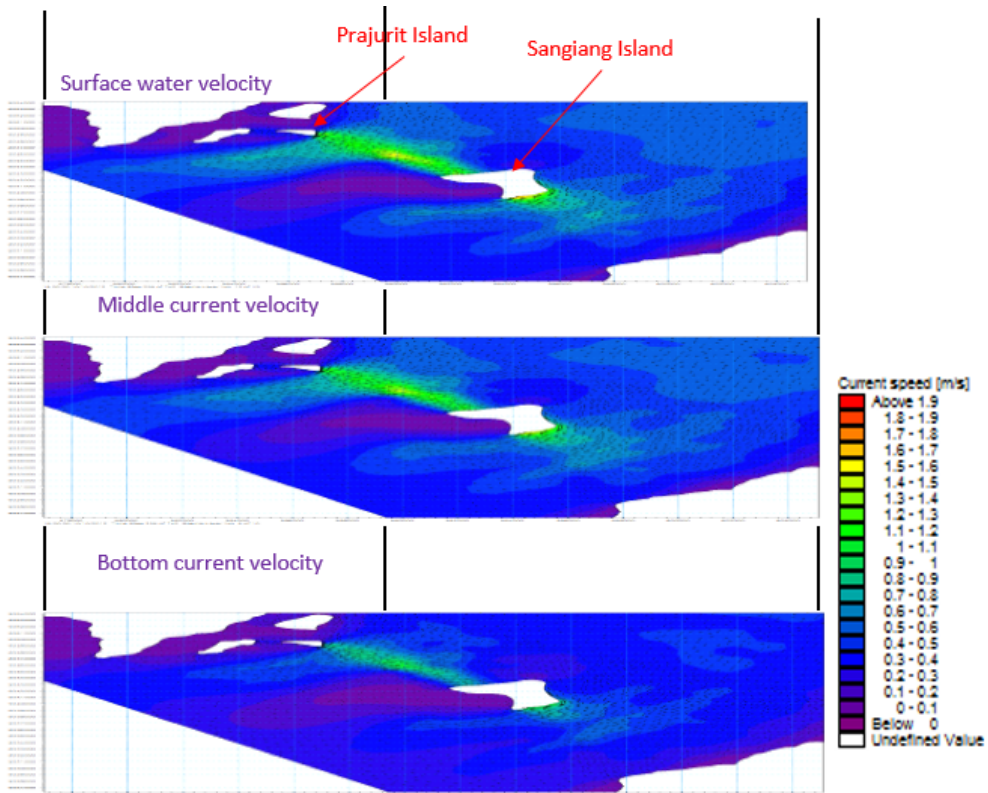


Figure 9. Current velocity of flood max in neap tide

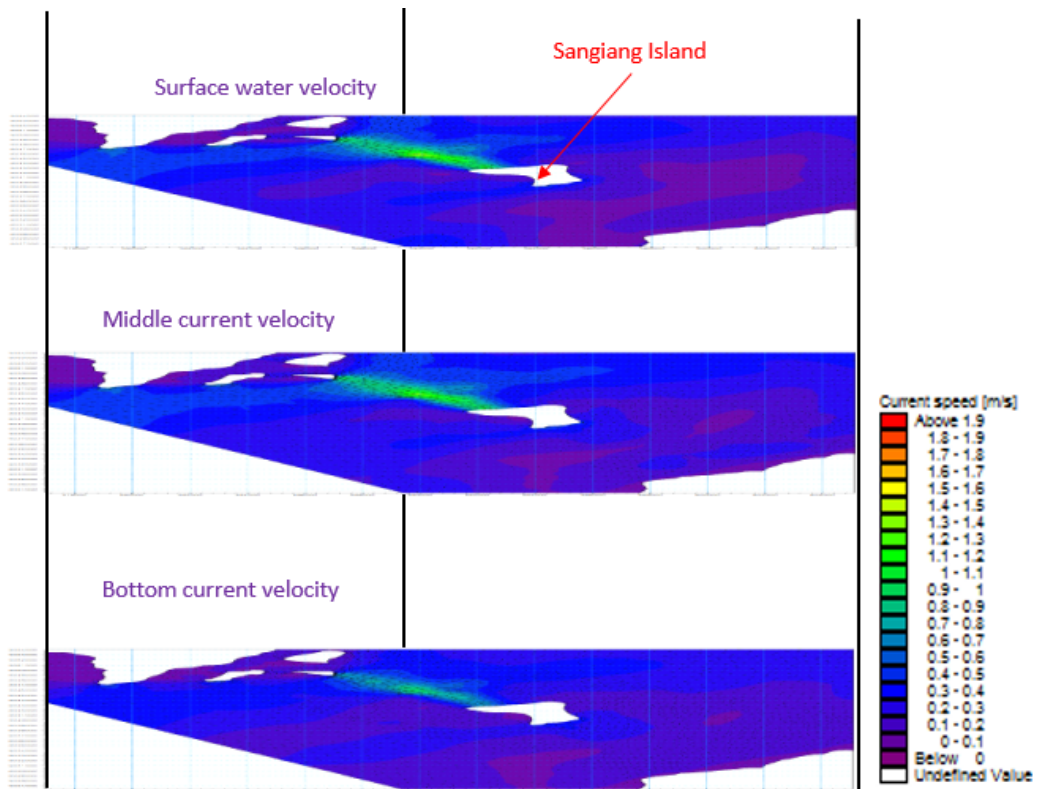


Figure 10. Current velocity of ebb max in neap tide

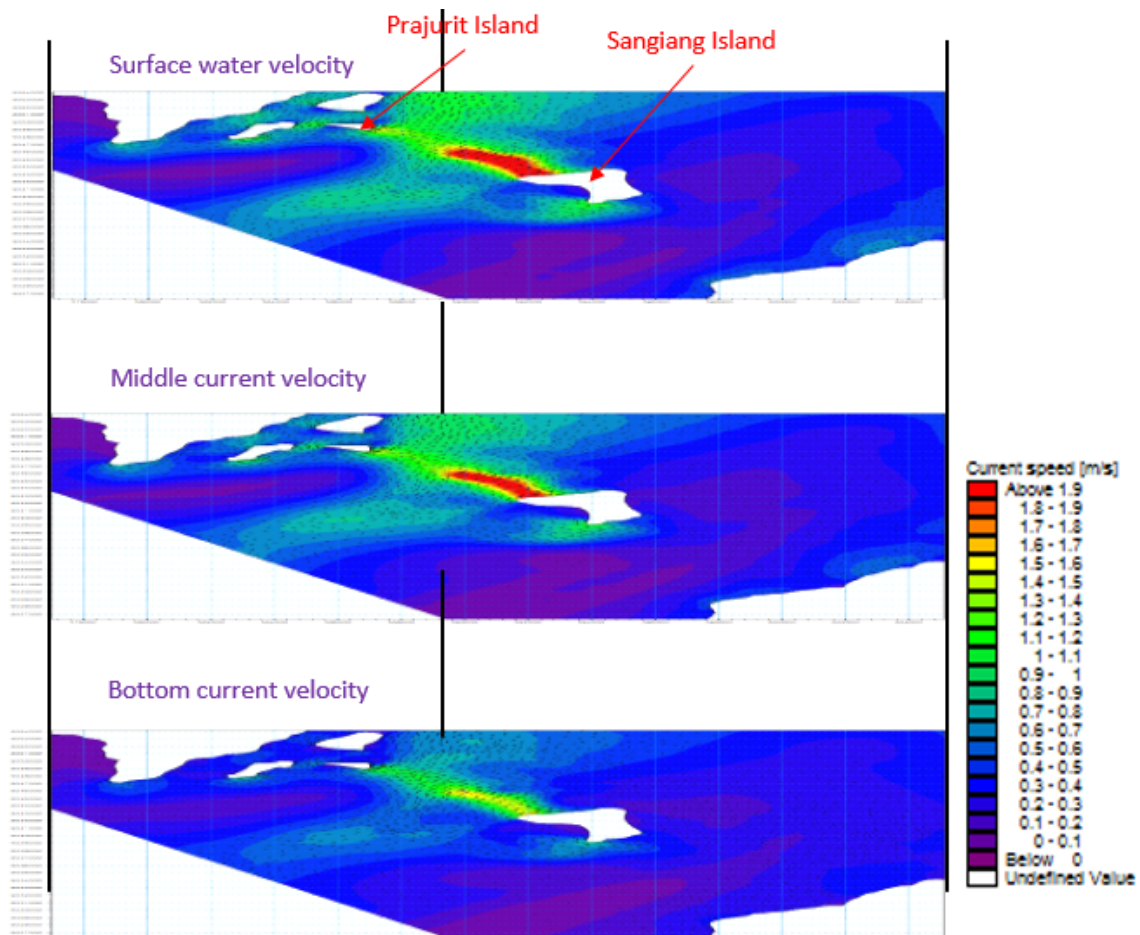


Figure 11. Current velocity of flood max in spring tide

vertical distribution of current velocity could be found at Figure 11 which it presents a dominant direction comes from the north-northeast to the south and some places experiencing swirls. Moreover, the higher velocity still occurred in the middle depth of water, especially in northwest Sangiang Island.

#### Current Condition at Ebb Max in Spring Tide

The next figure would be presented the current velocity condition in ebb max where it happened in 18<sup>th</sup> October 2012, 02:00 WIB. It is different with flood max, while in the ebb the highest current velocity is only about 1.3 m/sec and the average is 0.9 m/sec. In this situation, the highest current velocity occurred in southeast and western part of the Sangiang Island, Figure 12. The current direction drifts from the southwest-south to the north-northeast.

#### The Highest Current Velocity

Based on the hydrodynamic model, it could be seen the highest current velocity is happened at 17<sup>th</sup> October 2012, 23:00 WIB that velocity takes place 3 hours before ebb in the spring tide. If we compare that time to the maximum flood and ebb in the spring tide so it will be about 27 hours before ebb maximum and 34 hours before flood maximum. Figure 12 indicates the snapshot of the highest distribution of current velocity located in the Sangiang Island to the Prajurit Island and the southeast Sangiang Island. The average velocity in this snapshot is about 1.36 m/sec and the highest is 4.59 m/sec.

In term of construction of a bridge plan, it should be paid attention about area at risk and the time to avoid mobilize during construction. As can be seen in Figure 12, the white dashed line is the border of the area within current velocity more than 2 m/sec and total area  $\pm 16.5$  km<sup>2</sup>. Within this border, the shipping and construction activities should be avoided. In addition, time to construction should be avoided the time at least 48 hours before and after the flood-ebb maximum in the spring tide.

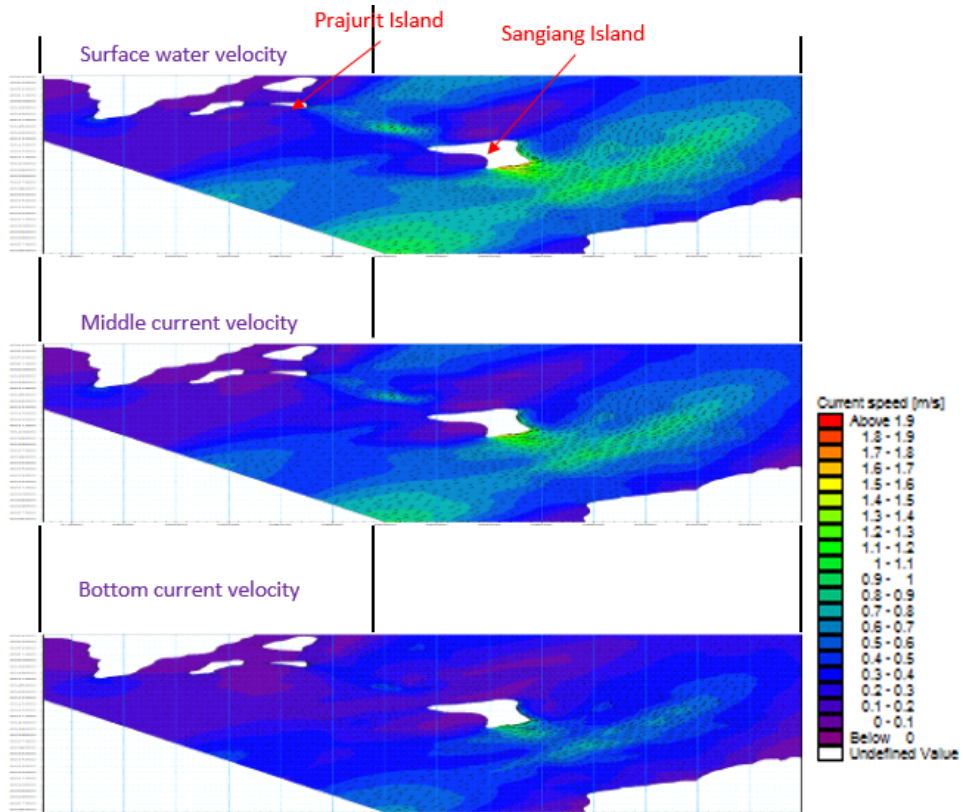


Figure 11. Current velocity of ebb max in spring tide

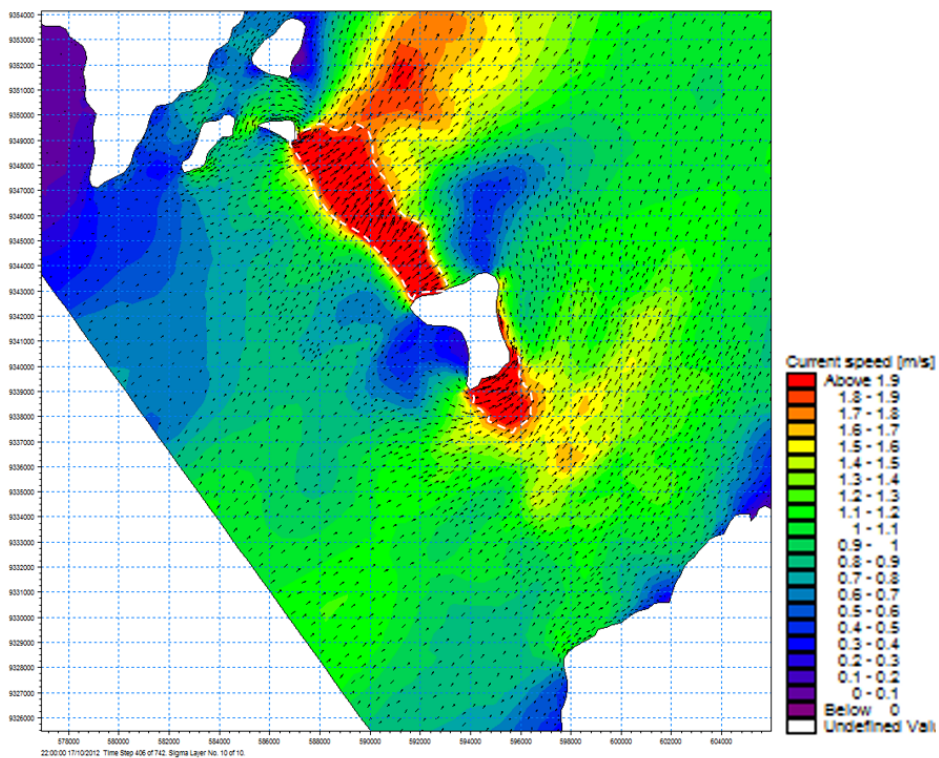


Figure 12. The highest current speed distribution

## CONCLUSION

The current velocity measurement along The Sunda Strait in the spring tide shows the highest current velocity of 2.63 m/sec occurred in 18<sup>th</sup> October 2012 at 16.30 WIB, when the vessel runs from southeast to northwest. It means the highest velocity was about 9.5 hours before the lowest water spring.

Based on a numerical model, the area of northwest Sangiang Island have a highest number of current velocity which is about 4.59 m/sec that it happened 3 hours before the ebb. Besides, the whirlpool is occurred not only in the northwest Sangiang Island but also at southern part of the island. Since the bridge plan is located along the Sunda Strait. Therefore, it should be paid attention to avoid the area that have a high velocity in the particularly tide time.

## ACKNOWLEDGEMENT

This paper was full supported by the Ministry of Energy and Mineral Resources especially Marine Geological Institute (MGI). Hence, the author would like to say thank to the Director of MGI and the personnel of RV Geomarin I.

## REFERENCES

- [1] Blumberg, A. F., and G. L. Mellor 1987, A description of a threedimensional coastal ocean circulation model, in Three-Dimensional Coastal Ocean Models, Coastal Estuarine Stud., vol. 4, edited by N. Heap, pp. 1 – 16, AGU, Washington, D. C.
- [2] DHI Water & Environment. 2007. Mike 21 FM HD Manual Book, Denmark.
- [3] Darwish, M.S., Moukalled, F., 2003. TVD schemes for unstructured grids. Int. J. Heat Mass Transfer 46, 599–611.
- [4] Gan, J., Li, H., Curchitser, E.N., and Haidvogel, D.B., 2006. Modeling South China Sea Circulation : Response to Seasonal Forcing Regimes, Journal of Gephysical Research, Vol. 111, C06034.
- [5] Hirsch, C., 1990. Numerical Computation of International and External Flows. 2<sup>nd</sup> ed., John Wiley & Sons, New York, USA
- [6] Jawahar P. and H. Kamath. (2000). A high-resolution procedure for Euler and Navier-Stokes computations on unstructured grids, Journal Comp. Physics, 164 (165-203)
- [7] King B. A. and E. B. Cooper (1993) Comparison of ship's heading determined from an array of GPS antennas with heading from conventional gyrocompass measurements. Deep-Sea Research I, 40, 2207-2216.
- [8] King B. A., Alderson S.G., and Cromwell, D (1996) Enhancement of shipboard ADCP data with DGPS position and GPS heading measurements. Deep-Sea Research I, Volume 43, No. 6. pp 937-947.
- [9] Astawa I. N., Laporan Penelitian Geologi Geofisika Kelautan dan Arus di Selat Sunda, Marine Geological Institute, Bandung
- [10] Munk, W., Anderson, E. (1948), Notes on the theory of the thermocline, Journal of Marine Research, 7, (276-295)
- [11] Padman,L.(2005) Tide Model Driver (TMD) Manual Available from [ftp://ftp.esr.org/pub/datasets/tmd/tmd\\_toolbox.zip](ftp://ftp.esr.org/pub/datasets/tmd/tmd_toolbox.zip)
- [12] Smagorinsky (1963), J. General Circulation Experiment with the Primitive Equations, Monthly Weather Review, 91, No.3, (99-164)
- [13] Susilohadi, Gaedicke. C., and Djajadihardja. Y., (2009) Structures and Sedimentary Deposition in The Sunda Strait, Indonesia. Tectonophysics Volume 467, Issues 1-4, pp 55-71
- [14] Szupiany, R.N., Amsler, M.L., Best, J.L., Parsons, D.R., 2007. A comparison of fixed and moving-vessel flow measurements with an acoustic Doppler profiler (aDp) in a large river. Journal of Hydraulic Engineering 133 (12), 1299e1309.
- [15] Warren, J.D and Peterson, B.J., 2007. Use of a 600-khz Acoustic Doppler Current Profile to measure estuarine bottom type, relative abundance of submerged aquatic vegetation, and eelgrass canopy height. Estuarine, Coastal and Shelf Science 72 (2007) 53-62
- [16] Wewetzer, S. F. K., Duck, R. W., & Anderson, J. M. (1999). Acoustic Doppler current profiler measurements in coastal and estuarine environments: examples from the Tay Estuary, Scotland. *Geomorphology*, 29(1-2), 21-30 doi: 10.1016/S0169-555X(99)00004-5
- [17] Wu, C.R., Chao, S.Y, and Hsu, C, 2007. Transient, Seasonal and Interannual Variability of the Taiwan Strait Current. Journal of Oceanography, Vol.63, pp.821 to 833, 2007